

Suppression of Ostwald ripening in $\text{In}_{0.5}\text{Ga}_{0.5}\text{As}$ quantum dots on a vicinal (100) substrate

Byung Don Min

Department of Physics, Korea University, Seoul 136-701, Korea

Yong Kim,* Eun Kyu Kim, and Suk-Ki Min

Semiconductor Materials Research Laboratory, Korea Institute of Science and Technology, P.O. Box 131, Cheongryang, Seoul 130-650, Korea

Mann Jang Park

Department of Physics, Korea University, Seoul 136-701, Korea

(Received 13 November 1997; revised manuscript received 23 January 1998)

A comparative study of the morphology of self-assembled $\text{In}_{0.5}\text{Ga}_{0.5}\text{As}$ quantum dots grown by atmospheric pressure metal-organic chemical vapor deposition on the exact (100) and 2° -off (100) GaAs substrates as a function of growth interruption time (0–1200 sec) is presented. The dots are randomly distributed on the exact (100) substrate, whereas the dots on the 2° -off (100) substrate are aligned along multiatomic steps. As the interruption time t is increased, the density of dots on the exact (100) substrate decreases and their average volume progressively increases with $\sim t^{3/4}$ dependence, indicating a regular Ostwald-ripening process. By contrast, the average volume of dots on the 2° -off (100) substrate saturates for interruption times over 200 sec and shows obvious suppression of ripening. In particular, the size of dots on the 2° -off (100) substrate is limited within the atomic terrace width (~ 55 nm). These results demonstrate that the density and size of dots could be controlled by interruption time and substrate miscut angle. [S0163-1829(98)04416-6]

Quantum dots (QD's) have received a great deal of attention due to their unique physical properties and optoelectronic device applications.¹ Self-assembled QD's utilizing a Stranski-Krastanow growth mode are attractive because they are formed as defect-free dots. These type of QD's have been achieved for highly strained material systems, including InGaAs/GaAs ,^{2–4} InAs/GaAs ,⁵ and $\text{In}_x\text{Al}_{1-x}\text{As}/\text{Al}_y\text{Ga}_{1-y}\text{As}$ (Refs. 6 and 7) by molecular beam epitaxy and metal-organic chemical-vapor deposition (MOCVD).

The growth of self-assembled QD's is initiated with two-dimensional (2D) layer growth. After a critical 2D layer thickness is reached, a structural transition toward the formation of three-dimensional QD's occurs because it is energetically favorable over planar growth.⁸ When the growth is interrupted after the structural transition, 3D dots experience an Ostwald ripening process, in which larger islands grow at the cost of smaller islands.⁹ It has been known that the size of the dots can depend on various parameters such as lattice mismatch, growth temperature, and III/V ratio.^{10,11} However, the importance of growth interruption time, particularly for MOCVD growth, has been overlooked. A recent study of the growth interruption effect on QD evolution showed an enlargement of dots as the interruption time is increased. This was attributed to an effect of mass transfer from the wetting layer.¹⁰ The evolution of dots was indirectly observed by photoluminescence measurements. However, a structural observation of dot evolution after growth interruption would be important because it provides an insight for designing a QD system. In particular, structural observation of QD evolution on a vicinal substrate would be interesting because QD formation is seriously affected by a miscut angle.¹²

In this work, the effect of Ostwald ripening during growth interruption on the formation and size variation of $\text{In}_x\text{Ga}_{1-x}\text{As}/\text{GaAs}$ dots is studied.

Self-assembled QD's were grown on exact and 2° -off (100) GaAs substrates tilted toward (010) by a vertical atmospheric pressure MOCVD Trimethylgallium (TMG), trimethylindium (TMI), and arsine (AsH_3) were used as source materials. The supply rates of TMG, TMI, and AsH_3 were 1.25, 0.99, and 223.1 $\mu\text{mol}/\text{min}$, respectively. Total flow rate of H_2 carrier gas was 5 standard liters per minute. Prior to growth, the substrates, which were loaded simultaneously side by side, were preannealed at 850°C for 10 min in arsine flow for deoxidation and step stabilization. Then 100 nm GaAs buffer layers were grown at 650°C with a low growth rate (~ 0.7 ML/s). Under this growth condition, a step flow growth mode was found for the buffer layer on the exact substrate and multiatomic steps with ~ 10 ML height were formed on the vicinal substrate. $\text{In}_{0.5}\text{Ga}_{0.5}\text{As}$ layers were grown on the GaAs buffer layers at 470°C with V/III of 100. The thickness of the $\text{In}_{0.5}\text{Ga}_{0.5}\text{As}$ layer was nominally 5 MLs. The actual composition can be different due to the indium segregation effect.¹³ After the growth of the $\text{In}_{0.5}\text{Ga}_{0.5}\text{As}$ epitaxial layers, the growth was interrupted from 0 to 1200 sec (0, 30, 60, 300, 600, and 1200 sec) and the samples were cooled down. Then $\text{In}_{0.5}\text{Ga}_{0.5}\text{As}$ surface morphologies were observed in air at room temperature by using atomic force microscopy (AFM).

Figure 1 shows a series of the AFM images of dots formed on the exact (100) and 2° -off (100) GaAs substrates with various interruption times. The upper set of figures [Figs. 1(a), 1(b), 1(c), and 1(d)] represents the images of the dots formed on the exact (100) GaAs substrate at the interruption times of 0, 30, 300, and 1200 sec, respectively. The lower set of figures [Figs. 1(e), 1(f), 1(g), and 1(h)] are the images of the dots formed on the 2° -off (100) GaAs substrate. For no interruption time (0 sec) [Figs. 1(a) and 1(e)]

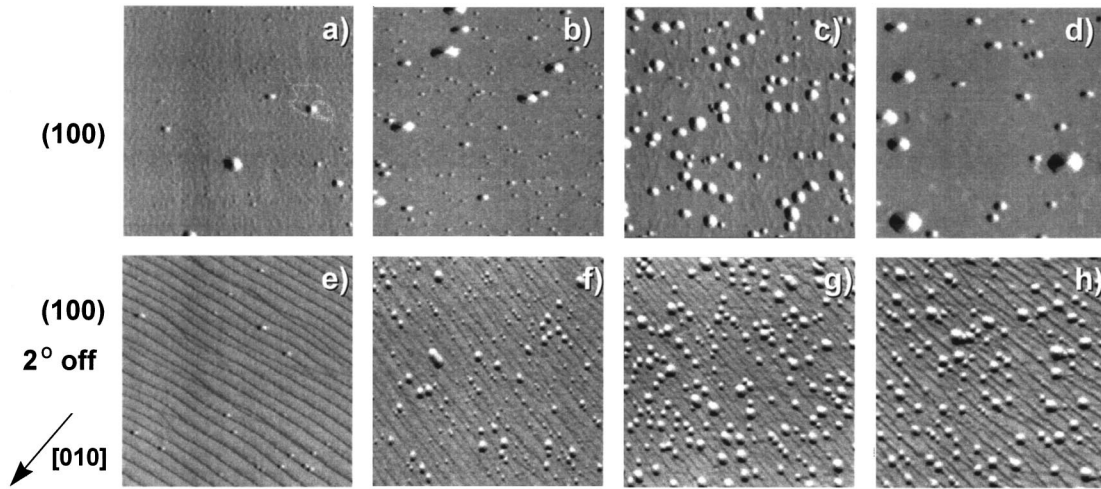


FIG. 1. $1 \times 1 \mu\text{m}^2$ atomic force microscope images with various growth interruption times. (a), (b), (c), and (d) (upper row) are the images of dots formed on the exact (100) substrate with interruption times of 0, 30, 300, and 1200 sec, respectively. (e), (f), (g), and (h) (lower row) are the images of dots formed on the 2° -off (100) substrate tilted toward the $\langle 010 \rangle$ direction with interruption times of 0, 30, 300, and 1200 sec, respectively.

the density of dots on the exact and 2° -off (100) GaAs substrate is low ($\sim 1 \times 10^9/\text{cm}^2$). As shown in Fig. 1(e), multi-atomic steps with ~ 55 nm wide atomic terraces are clearly visible. For interruption time of 30 sec [Figs. 1(b) and 1(f)], the dot densities on the two different substrates are increased to about $(1-3) \times 10^{10}/\text{cm}^2$. As shown in the AFM images, small, not fully developed QD's appear with larger islands indicating a clear bimodal size distribution. The histogram analyses as displayed in Fig. 2 shows the clear evidence of the bimodal size distribution (mode I for smaller dots and mode II with dispersed distribution for larger dots). The analyses were done for the samples with 30 sec interruption time that were shown in Figs. 1(b) and 1(f). The size dispersions, σ of smaller dot groups (mode I distributions), were 10.4% for the sample on the 2° -off (100) substrate and 11.8% for the sample on the exact (100) substrate. Those size dispersions are comparable to the lowest dispersion reported so far.^{5,12} The dots density ($\sim 3 \times 10^{10}/\text{cm}^2$) on the 2° -off (100) substrate is higher than that ($\sim 1 \times 10^{10}/\text{cm}^2$) on the exact (100) substrate, reflecting the larger number of nucleation sites at step edges on the vicinal surface. For interruption times over 300 sec, the dot density on the exact substrates decreases and the dot size increases due to Ostwald ripening. However, strikingly, dots on the vicinal (100) substrate do *not* show such an obvious density reduction and ripening process. The AFM images of dots on the vicinal substrate show the alignment of every dot along the step edges. This indicates the preferential nucleation of dots on the step edges and leads to the QD alignment along the steps. This result is in agreement with previous reports on heterogeneous nucleation.^{3,4,12}

The statistical distribution of dot sizes on the two different substrates are analyzed by plotting histograms as shown in Fig. 3.¹⁴ The left column represents the set of histograms of QD's on the exact substrate, while the right column shows the set of histograms of QD's on the vicinal substrate. The dotted line indicates the average terrace width of the 2° -off (100) substrate. As shown in the left column, QD size dispersion increases with their average size, which occurs when increasing the interruption time. However, no obvious in-

crease of the size dispersion of QD's on the vicinal substrate is observed. Furthermore, the dot size on the 2° -off (100) substrate is always less than the terrace width, implying the existence of a driving force for the suppression of ripening.

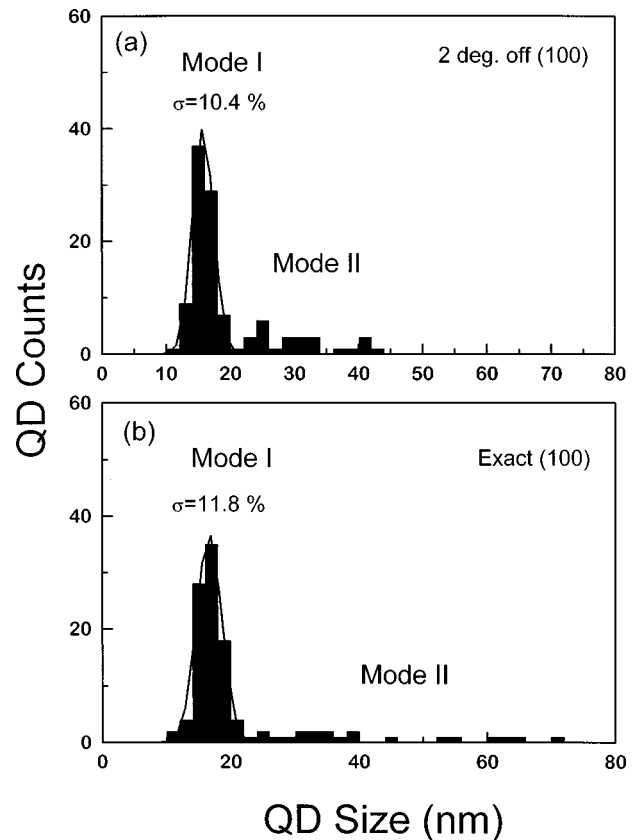


FIG. 2. Histograms of dot size distribution with the growth interruption time of 30 sec for (a) $\text{In}_x\text{Ga}_{1-x}\text{As}$ quantum dots on the 2° -off (100) GaAs substrates, and (b) the exact (100) GaAs substrate. The Gaussian fits for size dispersion analysis are shown as solid lines. The bimodal size distributions (mode I for smaller dots and mode II with the dispersed distribution for larger dots) are evident for both samples.

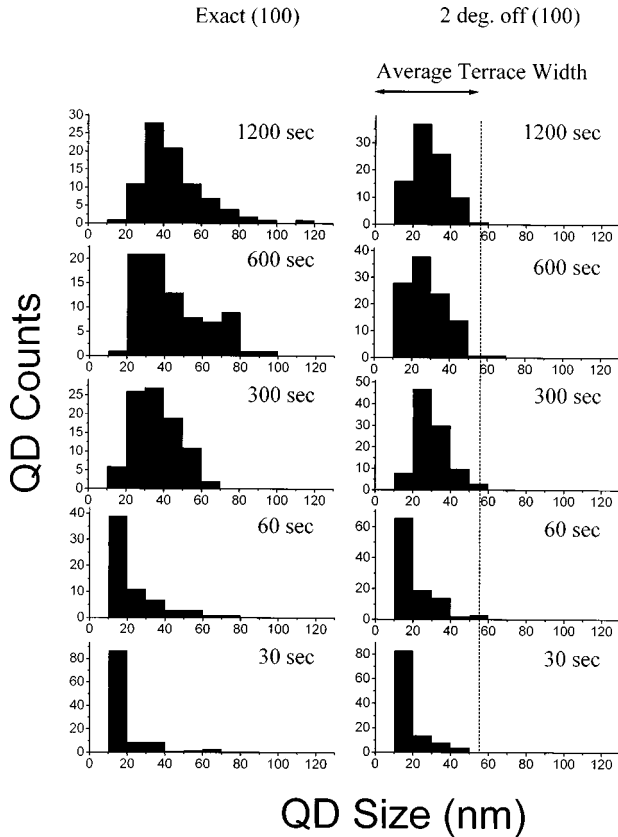


FIG. 3. Histograms of dot size distribution with various growth interruption times (0~1200 sec) for $\text{In}_x\text{Ga}_{1-x}\text{As}$ quantum dots on exact (left column) and 2° -off (100) GaAs substrates (right column). The dotted line along the set of data in the right column indicates the average terrace width (~ 55 nm).

Figures 4(a) and 4(b) show the total and average volume of QD's per unit area ($1 \mu\text{m}^2$) on the exact and 2° -off substrates as a function of the interruption time. The volume of an individual dot is estimated by using the measured height and lateral size assuming a spherical cap geometry of the dot.⁵ We believe that this assumption is valid and representative for our experimental data. As shown in Fig. 4(a), at interruption times from 0 to 60 sec, the total volume of dots on both substrates rapidly increases with increasing interruption time. This indicates that dot formation is proceeding at the expense of the $\text{In}_x\text{Ga}_{1-x}\text{As}$ wetting layer. This finding supports the hypothesis of the mass transfer from the supercritically thick wetting layer during the initial growth interruption.¹⁵ In this case, QD's may act as catalysts to decompose the supercritically thick wetting layer. Surprisingly, total QD volumes are saturated at $\sim 1 \times 10^6 \text{ nm}^3/\mu\text{m}^2$ regardless of the substrate miscut angle. This result implies that total QD volume is controlled not by kinetics but by thermodynamics. No loss of total QD volume is found even at larger interruption times, indicative of negligible thermal desorption during the adatom diffusion at the growth temperature of 470°C . The average volume [Fig. 4(b)] of dots on the exact substrate increases with increasing interruption time. Fits to the data are made with the scaling theory for the Ostwald ripening.¹⁶ By the kinetics of the ripening process, energy minimization represents the driving force for cluster growth. The total surface energy of a system is decreased

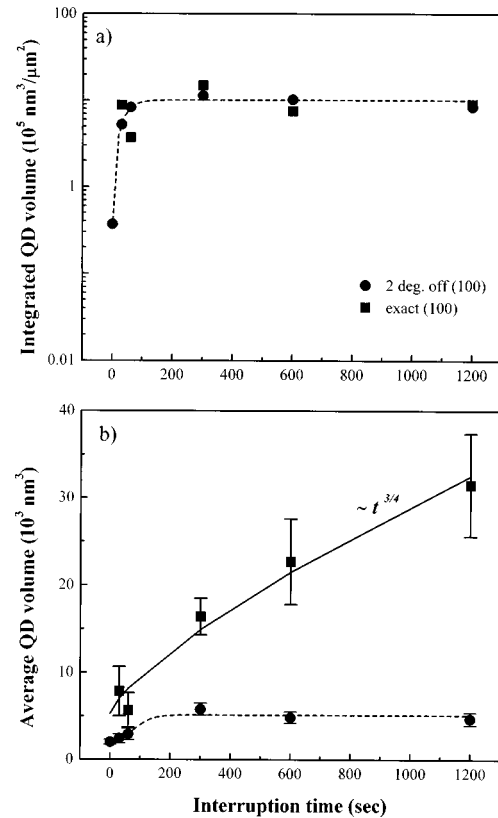


FIG. 4. (a) Total and (b) average volumes of $\text{In}_x\text{Ga}_{1-x}\text{As}$ quantum dots as a function of interruption time. The solid line in (b) is a fit to $\sim t^{3/4}$ functional dependence. The dotted lines in (a) and (b) are sigmoidal function fits to guide the eye.

when small particles combine to form larger clusters with no loss of mass.¹⁷ When the dots are formed with a hemisphere of radius r , r would increase with interruption time t at a rate of $t^{1/4}$. That is, the volume V should increase at a rate of $t^{3/4}$.¹⁶ Successful fits can be found in Fig. 4(b). $t^{3/4}$ dependence of the volume implies that the ripening is diffusion limited. After the consumption of part of the wetting layer, the ripening effect starts on the exact substrate. However, it is noteworthy that the initial mass transfer takes place during the very early stage of the growth interruption. Therefore, in conjunction with the total QD volume analysis [Fig. 4(a)], a redshift of QD luminescence with the growth interruption time, previously assessed as the mass transfer from wetting layer,¹⁰ would be mainly due to a ripening effect.

The average volume of dots on the 2° -off (100) substrate are increased initially but saturated at larger interruption times over ~ 200 sec. A dotted line in Fig. 4(b) represents a sigmoidal fit to guide the eye. The initial increase of the average QD volume on the vicinal substrate is likely due to the same origin as QD evolution on the exact substrate (i.e., mass transfer from the supercritically thick wetting layer). However, in the case of the dots on the vicinal substrate, migration of adatoms from a terrace to another terrace across the step for incorporation to dots may be prohibited at this low growth temperature ($\sim 470^\circ\text{C}$) due to the energy barrier (i.e., Schwoebel barrier) formed at the step kink.¹⁸⁻²⁰ Therefore, the obvious effect of steps is to reduce the reservoir of atoms available for dot growth. During the initial stage of growth interruption (approximately less than ~ 200 sec in

our experiment), regardless of substrate choice, QD's seem to grow by collecting atoms from surrounding the wetting layer as observed in Fig. 4(b). However, the key point is that atoms will have to diffuse further away than they otherwise would in the absence of steps. This effect seems to offer more chance to grow to smaller dots and thereby results in relatively uniform size distribution of QD's on vicinal substrates. However, a complete solution of the diffusion equation of atoms on the stepped surface will provide the quantitative verification of our argument presented in this paper. In our experiment, the average terrace width was ~ 55 nm. However, by increasing the substrate misorientation angle, the average terrace width can be reduced further. In this case, uniform and high density QD's with larger quantum confinement can be fabricated. For interruption times over 200 sec, the Ostwald ripening effect is suppressed probably due to the strong binding of QD's at step edges. We believe that this is an important result because the control of interruption time

in conjunction with the misorientation angle can be directed toward the control of the density and size of dots.

To conclude, we have studied the self-assembling behavior of $\text{In}_x\text{Ga}_{1-x}\text{As}$ quantum dots on exact and 2° -off (100) GaAs substrates as a function of growth interruption time. We found that the enlargement of dot size on the vicinal surface is not increased over a critical size (i.e., terrace width). This is in contrast with the result for dots on the exact substrate that shows regular Ostwald ripening. From this result, we expect to obtain $\text{In}_x\text{Ga}_{1-x}\text{As}$ quantum dots with low size dispersion and high density by properly choosing the interruption time and substrate orientation.

The authors would like to thank Dr. R. Leon for a critical reading of the manuscript and for fruitful discussions. This work has been supported in part by the K-2000 Project under Contract No. 2V00211 and the Miraewoncheon Project under Contract No. 2N15920.

*Author to whom correspondence should be addressed. Electronic address: yongkim@kistmail.kist.re.kr

¹Y. Arakawa and H. Sakaki, *Appl. Phys. Lett.* **40**, 939 (1982).

²F. Heinrichsdorff, A. Krost, M. Grundmann, D. Bimberg, A. Kosogov, and P. Werner, *Appl. Phys. Lett.* **68**, 3284 (1996).

³J. Oshinowo, M. Nishioka, S. Ishida, and Y. Arakawa, *Jpn. J. Appl. Phys., Part 2* **33**, L1634 (1994).

⁴M. Kitamura, M. Nishioka, J. Oshinowo, and Y. Arakawa, *Appl. Phys. Lett.* **66**, 3369 (1995).

⁵D. Leonard, K. Pond, and P. M. Petroff, *Phys. Rev. B* **50**, 11 687 (1994).

⁶S. Fafard, R. Leon, D. Leonard, J. L. Merz, and P. M. Petroff, *Phys. Rev. B* **50**, 8086 (1994).

⁷R. Leon, S. Fafard, D. Leonard, J. L. Merz, and P. M. Petroff, *Appl. Phys. Lett.* **67**, 521 (1995).

⁸Y. Chen and J. Washburn, *Phys. Rev. Lett.* **77**, 4046 (1996).

⁹N. Carlsson, K. Georgsson, L. Montelius, L. Samuelson, W. Seifert, and R. Wallenberg, *J. Cryst. Growth* **156**, 23 (1995).

¹⁰F. Heinrichsdorff, A. Krost, M. Grundmann, D. Bimberg, F. Bertram, J. Crysten, A. Kosogov, and P. Werner, *J. Cryst. Growth* **170**, 568 (1997).

¹¹M. Geiger, A. Bauknecht, F. Adler, H. Schweiger, and F. Scholz,

J. Cryst. Growth **170**, 558 (1997).

¹²R. Leon, T. J. Senden, Yong Kim, C. Jagadish, and A. Clark, *Phys. Rev. Lett.* **78**, 4942 (1997).

¹³N. Grandjean, J. Massies, and O. Tottereau, *Phys. Rev. B* **55**, R10 189 (1997).

¹⁴We choose 10 nm bins for more clear comparison between 10 histograms. In contrast, we choose 2 nm bins for the histograms shown in Fig. 2 in order to display more evident bimodal size distributions.

¹⁵W. Seifert, N. Carlsson, J. Johansson, M.-E. Pistol, and L. Samuelson, *J. Cryst. Growth* **170**, 39 (1997).

¹⁶M. Zinke-Allmang, L. C. Feldman, and S. Nakahara, *Appl. Phys. Lett.* **51**, 975 (1987).

¹⁷K. N. Tu, J. W. Mayer, and L. C. Feldman, *Electronic Thin Film Science for Electrical Engineers and Materials Scientists* (Macmillan, New York, 1992), Chap. 5.

¹⁸R. L. Schwoebel and E. J. Shipsey, *J. Appl. Phys.* **37**, 3682 (1966).

¹⁹Y. Tokura, H. Saito, and T. Fukui, *J. Cryst. Growth* **94**, 46 (1989).

²⁰F. W. Sinden and L. C. Feldman, *J. Appl. Phys.* **67**, 745 (1990).